

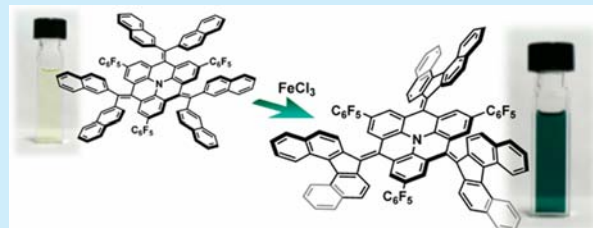
# Heterotriangulenes $\pi$ -Expanded at Bridging Positions

Chih-Ming Chou,<sup>†</sup> Shohei Saito,<sup>†</sup> and Shigehiro Yamaguchi<sup>\*,†,‡</sup>

<sup>†</sup>Department of Chemistry, Graduate School of Science, and <sup>‡</sup>Institute of Transformative Bio-Molecules (WPI-ITbM), Nagoya University, Furo, Chikusa, Nagoya 464-8602, Japan

**S** Supporting Information

**ABSTRACT:** A series of nitrogen-containing heterotriangulenes expanded at the bridging positions has been synthesized. Among them, a dibenzo[*c,g*]fluorenylidene-substituted derivative has a highly twisted conformation for the overcrowded alkene moieties, which impart a highly electron-accepting character to the electron-donating heterotriangulene skeleton and thereby an NIR absorption as well as multiredox properties with a low reduction potential.



Heterotriangulenes with a planar nitrogen atom at the center are simple and attractive building blocks for functional organic materials.<sup>1–9</sup> A representative example is the carbonyl-bridged heterotriangulene **1** (Figure 1).<sup>1</sup> Several derivatives

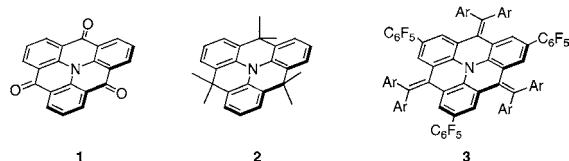


**Figure 1.** Chemical structures of heterotriangulene derivatives.

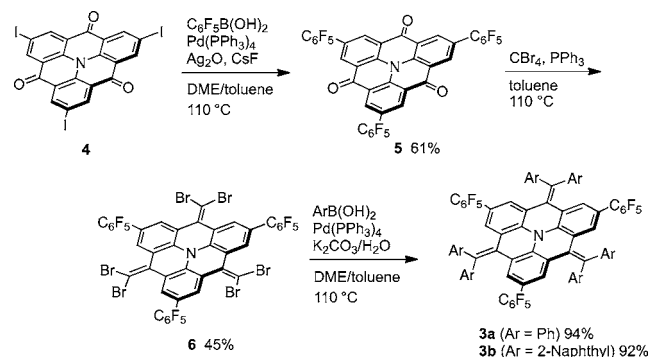
functionalized at the phenyl rings with *n*-dodecyl or 4-alkoxyphenylethynyl groups were synthesized, and their self-assembly behavior to form nanowires or microrods was reported.<sup>2,3</sup> Heterotriangulene-based dendrimers with carbazole moieties were also studied as a potential material for organic light emitting diodes (OLEDs).<sup>4</sup> One issue regarding their molecular design is the poor solubility of the core triangulene skeleton in common organic solvents, which limits the applications in organic electronics. In this regard, the replacement of the carbonyl bridging moieties in **1** with  $sp^3$ -hybridized dimethyl-methylene groups imparts a better material processability. Compound **2** thus developed has been utilized as a promising building block for the hole-transporting or -injecting materials with a high thermal stability in OLEDs, materials with large two-photon absorption cross section, and materials for dye-sensitized solar cells.<sup>5–8</sup>

Heterotriangulene **2** has the intrinsic electronic nature of triphenylamine. The expansion of the skeleton at the para-positions of the three phenyl rings is a rational way to produce electron-donating materials. In addition, the heterotriangulene is a potential building block for heteroatom-embedded polycyclic aromatic hydrocarbons, ultimately including heteroatom-doped graphene flakes.<sup>10</sup> The first step to this end should be expansion of  $\pi$  conjugation at the bridging moieties between the phenyl rings. However, no derivative has yet been studied from this

point of view.<sup>11</sup> We now report the synthesis of a series of heterotriangulenes **3**  $\pi$ -expanded at the bridging positions. In particular, we disclose the significant impacts of different  $\pi$ -expansion modes, the introduction of highly distorted C=C double bonds and the unsymmetrical annulation with more fused benzene rings, on their structures and electronic properties.

For the synthesis of  $\pi$ -expanded heterotriangulenes, we first synthesized an iodinated compound **4** as a key precursor which was prepared according to the literature (Scheme 1).<sup>4</sup> A  $C_6F_5$ -

## Scheme 1. Synthesis of $\pi$ -Expanded Heterotriangulenes



substituted **5** was obtained by the Pd-catalyzed Suzuki–Miyaura coupling of **4** with pentafluorophenylboronic acid in 61% yield.<sup>12</sup> The introduction of the  $C_6F_5$  groups increased not only the solubility but also the reactivity of the carbonyl functionality for the next reaction. Thus, the carbonyl groups were converted to the C=C double bonds by carrying out the 3-fold Corey–Fuchs reaction, which is useful for expanding  $\pi$ -systems.<sup>13</sup> A hexabrominated product **6** was successfully obtained in 45% yield. This compound was further transformed by the Suzuki–Miyaura coupling with phenylboronic acid or 2-naphthylboronic

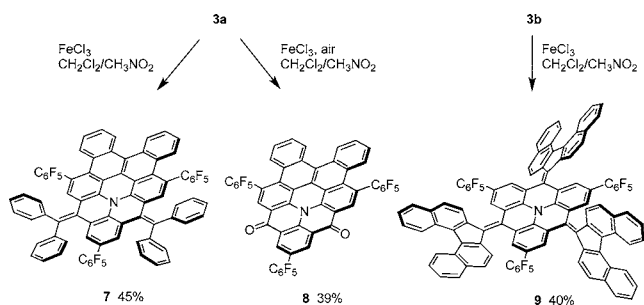
**Received:** April 5, 2014

**Published:** May 22, 2014

acid to the corresponding 6-fold coupling products **3a** and **3b** in 94 and 92% yields, respectively.

Compound **3a** was subjected to typical Scholl reaction conditions, namely the treatment with an excess amount (12 equiv) of  $\text{FeCl}_3$  in  $\text{CH}_2\text{Cl}_2/\text{CH}_3\text{NO}_2$  degassed with argon at  $0^\circ\text{C}$  for 30 min (Scheme 2).<sup>14</sup> A 10-ring-fused compound **7** was

### Scheme 2. Dehydrogenative Coupling of **3**



isolated as the main product in 45% yield. Notably, when the reaction was conducted in the presence of air, a dicarbonyl-substituted 10-ring-fused system **8** was obtained in 39% yield instead of **7**. This compound is likely produced by a [2 + 2] cycloaddition of singlet oxygen<sup>15</sup> to the olefin moieties in **7**, which is followed by C–C bond cleavage. Although we also attempted the dehydrogenative annulation of **3a** and the partially cyclized **7** using DDQ/Lewis acids or photocyclization methods, the reactions only produced unidentified complex mixtures. In contrast, when **3b** was employed as a substrate for the reaction with  $\text{FeCl}_3$  at  $0^\circ\text{C}$ , the dehydrogenative coupling smoothly took place at the naphthyl groups to give a dibenzo[*c,g*]-fluorenylidene-substituted heterotriangulene **9** as the main product in 40% yield. The low aromaticity of the naphthyl groups may facilitate the reaction. All the  $\pi$ -expanded heterotriangulenes **3a**, **3b**, **7**, **8**, and **9** have good solubilities in the common organic solvents, such as toluene,  $\text{Et}_2\text{O}$ , THF, and  $\text{CH}_2\text{Cl}_2$ , even at room temperature. For example, the solubilities of **3b** and **9** in  $\text{CH}_2\text{Cl}_2$  are 25.3 and 23.0 mg/mL, respectively.

Single crystals of **3a**, **7**, and **9** suitable for the X-ray diffraction analysis were obtained by a vapor diffusion method in different solvent systems (Figure 2 and Supporting Information). There

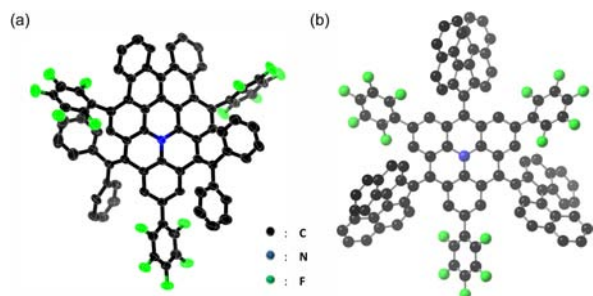


**Figure 2.** (a) Crystal structure of **7** and (b) DFT-optimized structure of **9** calculated at the B3LYP/6-31G\* level of theory.

are several notable features in their crystal structures. First, whereas the 3-fold bridged triphenylamine core generally takes a planar structure,<sup>1,2</sup> that in **3a** has a bowl-shaped structure (Figure S1, Supporting Information). The sum of the C–N–C angles is  $351.8^\circ$ , and the N–C bond distances are 1.417(3)–1.425(2) Å, which are significantly elongated from the ordinary  $\text{Csp}^2\text{–N}$

bond length of 1.36 Å.<sup>16</sup> The bowl depth, the distance between the nitrogen atom and the plane defined by three para-carbon atoms of the benzene rings, is 1.1 Å. This result demonstrates that this planarized skeleton still has tolerance toward the structural deformation. A similar bowl-shaped structure is also reported for analogous bridged triphenylborane derivatives, although they take the bowl-shaped structure only in the excited state or in the one electron-reduced state.<sup>17</sup> Second, there is severe steric congestion between the diarylvinyldene moieties and the  $\text{C}_6\text{F}_5$  groups. As a consequence, the three vinyldene moieties in **3a** significantly deviate in the same direction, while the two vinyldene moieties in **7** are distorted in the opposite direction (Figure 2a and Figure S3, Supporting Information). This steric repulsion is likely responsible for the bowl-shaped structure in **3a**. Third, in the structure of **9**, the three dibenzo[*c,g*]fluorenylidene groups all adapt twisted overcrowded alkene conformations (Figure 2b and Figure S4, Supporting Information). The unit cell consists of five crystallographically independent molecules, all of which take the twisted alkene conformations similar to each other. This structure is worth noting since common overcrowded alkenes, like 9,9'-bi-(fluorenylidene), tend to have a folded structure as the more stable conformer compared to the twisted conformer.<sup>18</sup> The DFT (B3LYP/6-311G\*\*) structure optimization indicated that the structure with the twisted overcrowded alkene geometries is more stable than the folded congener by 4.9 kcal mol<sup>−1</sup> in zero-point corrected energies. This result suggests that the twist of the alkene units is not due to a packing force. The variable temperature <sup>1</sup>H NMR spectra in the range of 25–100 °C did not show a significant change (Figure S16, Supporting Information), suggesting that a high energy barrier for the structural change between the twisted and folded conformers suppresses the formation of the folded one or that the amount of folded species is negligible in the thermal equilibrium. The steric repulsion between the planar dibenzo[*c,g*]fluorenyl groups and the  $\text{C}_6\text{F}_5$  groups is again likely responsible for this structure, while the central triphenylamine core has a relatively planar geometry. This highly distorted structure gives rise to intriguing photophysical properties (vide infra).

The expansion of the  $\pi$  skeleton at the bridging moieties significantly alters the photophysical properties. The absorption and fluorescence data in  $\text{CH}_2\text{Cl}_2$  for **3** and **7–9** are summarized in Table 1, together with that of **2**<sup>6c</sup> for comparison. The 3-fold vinyldene-expanded **3a** and **3b** have the respective longest absorption maximum wavelengths ( $\lambda_{\text{abs}}$ ) at 377 and 397 nm, which are red-shifted by 76 and 96 nm from **2** ( $\lambda_{\text{abs}} = 301$  nm), respectively. Compound **7** with a dibenzochrysene substructure shows a more red-shifted absorption band with the  $\lambda_{\text{abs}}$  of 471 nm. More notably, the dibenzo[*c,g*]fluorenylidene-expanded derivative **9** has a broad absorption band that reaches the near-infrared (NIR) region with the  $\lambda_{\text{abs}}$  of 797 nm (Figure 3).

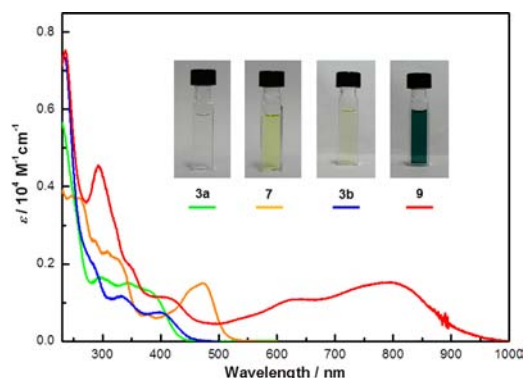
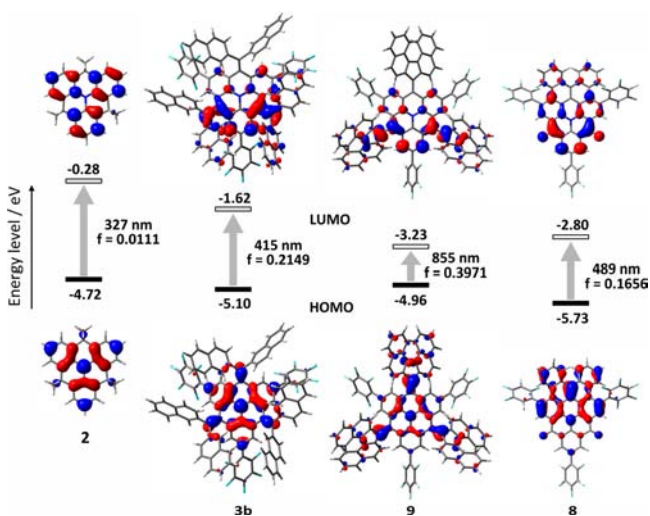
To rationalize the significant impact of the  $\pi$  expansion on the absorption properties, we conducted DFT structural optimization and TD-DFT calculations at the B3LYP/6-31G\* level of theory.<sup>19</sup> Figure 4 shows a comparison of the electronic structures among **2**, **3b**, **9**, and **8** (Figures S10–15, Supporting Information). For the TD-DFT calculation of **9**, the optimized geometry with the twisted conformation for the three fluorenylidene moieties was employed.

The HOMO of **3b** is delocalized in the central triphenylamine core with the contribution of the three vinyldene bridging moieties. Despite the expansion of the  $\pi$  conjugation, the HOMO level of **3b** is 0.38 eV lower than that of **2**, indicative of

**Table 1. Photophysical and Electrochemical Properties of Heterotriangulene Derivatives**

compd	photophysical properties in CH <sub>2</sub> Cl <sub>2</sub>			redox potential	
	$\lambda_{\text{abs}}^a$ (nm)	$\log \epsilon^b$ (M <sup>-1</sup> cm <sup>-1</sup> )	$\lambda_{\text{em}}^c$ (nm)	$\Phi_f^d$	
2 <sup>f</sup>	301		416		
3a	377	4.36	449	g	0.40
3b	397	4.43	490	g	0.39
7	471	4.50	517	g	0.20
8	530	4.26	569	0.20	1.02
9	797	4.57	i	g	0.30

<sup>a</sup>Only the longest absorption maxima are shown. <sup>b</sup>Molar extinction coefficient at the longest absorption maximum. <sup>c</sup>Emission maxima. <sup>d</sup>Absolute fluorescence quantum yield determined by a calibrated integrating sphere system within errors of  $\pm 3\%$ . <sup>e</sup>Determined by cyclic voltammetry with Bu<sub>4</sub>NPF<sub>6</sub> (0.1 M) at a scan rate of 0.1 V s<sup>-1</sup>. Potentials are given against the ferrocene/ferrocenium couple. The first oxidation and reduction potentials in CH<sub>2</sub>Cl<sub>2</sub> are shown, except for the reduction potentials of 3a, 3b, and 7 in THF. <sup>f</sup>Reference 6c. <sup>g</sup>Below 0.01. <sup>h</sup>Irreversible redox waves were observed. Peak potentials are shown. <sup>i</sup>Not observed.

**Figure 3.** UV-vis absorption spectra of 3a, 3b, 7, and 9 measured in CH<sub>2</sub>Cl<sub>2</sub>. Inset: photographs of their CH<sub>2</sub>Cl<sub>2</sub> solutions.**Figure 4.** Energy levels of the Kohn-Sham HOMOs and LUMOs for 2, 3b, 9, and 8 with the transition energies and oscillator strengths calculated at the B3LYP/6-31G\* level.

the electron-withdrawing effect of the bridging moieties. In contrast, the characteristics of the LUMOs for 3b and 2 are totally different from each other, the former of which is mainly

localized on the vinylidene moieties. The highly distorted geometries decreases the  $\pi^*$  orbital of the double bond moieties, resulting in the significant decrease in the LUMO level from 2 to 3b by 1.34 eV. As a result, 3b has the HOMO-LUMO transition band with the lower energy compared to that for 2. In addition, it is also noteworthy that the intramolecular charge transfer character in the HOMO-LUMO transition for 3b results in the significant increase in the oscillator strength ( $f = 0.215$ ) compared to 2 ( $f = 0.0111$ ), which is also an important outcome for the expansion of  $\pi$  skeleton with the three vinylidene moieties.

The ring closure from 3b to 9 further alters the electronic structure to a considerable extent. The formation of the fluorenylidene bridges increases the contribution of the vinylidene moieties to the HOMO delocalization, resulting in a slight increase in the HOMO level by 0.14 eV. A more dramatic change is suggested in the LUMO level from 3b to 9 by 1.61 eV due to the more significant distortion of the olefin moieties.

As a result, the dibenzo[*c,g*]fluorenylidene moieties act as the strong electron-accepting moieties, resulting in the significantly lower transition energy of 1.45 eV, consistent with the experimentally observed NIR absorption band.

In the fluorescence spectra, while the diarylvinylidene-substituted heterotriangulenes 3a, 3b, and 7 only show a faint fluorescence, the dibenzo[*c,g*]fluorenylidene-substituted 9 does not show any fluorescence. The weak or nonfluorescence characteristics are likely due to the highly distorted structure of the olefin moieties, which may accelerate the nonradiative decay process from the lowest excited singlet state. In contrast, the 10-ring-fused compound 8 with a rigid skeleton shows a relatively intense yellow emission with the maximum wavelength of 569 nm in CH<sub>2</sub>Cl<sub>2</sub>. The fluorescence quantum yield ( $\Phi_f$ ) is 0.20. Its fluorescence property depends on the solvents. While the compound shows a very small Stokes shift of 246 cm<sup>-1</sup> in cyclohexane, it increases to 1692 cm<sup>-1</sup> in DMF (Figure S6, Supporting Information). The Lippert-Mataga plot of the Stokes shift as a function of the solvent orientation polarizability shows a good linear relationship. The dipole moment change ( $\Delta\mu_{e-g}$ ) value between the ground state and the excited state is 13.6 D, while the calculated dipole moment in the ground state in the gas phase is 5.76 D. The DFT calculation of 8 revealed that while the HOMO is mainly delocalized on the dibenzochrysene moiety, the LUMO has a major contribution from the heterotriangulene with the dicarbonyl-substituted structure. The intramolecular charge transfer character gives rise to the large dipole moment change  $\Delta\mu_{e-g}$ .

The other notable feature of the expanded heterotriangulene is its multiredox properties. Their electrochemical properties were investigated by cyclic voltammetry (Table 1). As the representative compounds, the cyclic voltammograms of 3b, 8, and 9 are shown in Figure 5, among which the latter two compounds show reversible multistep redox waves for both the oxidation and reduction. In comparison with the dinaphthylvinylidene-substituted 3b, the ring closure to the dibenzofluorenylidene substructure in 9 results in the increased reversibility of the oxidation process and, more importantly, the significant positive shift of the reduction potentials. The half redox potential for the first reduction is -1.13 V (vs Fc/Fc<sup>+</sup>), which is comparable to that of C<sub>60</sub> (-1.0 V vs Fc/Fc<sup>+</sup>),<sup>20</sup> a representative electron-accepting compound. The differential pulse voltammetry study demonstrated that the first reduction process involves the two-electron reduction in one step. This compound can be reduced up to a tetraanion with a high reversibility,



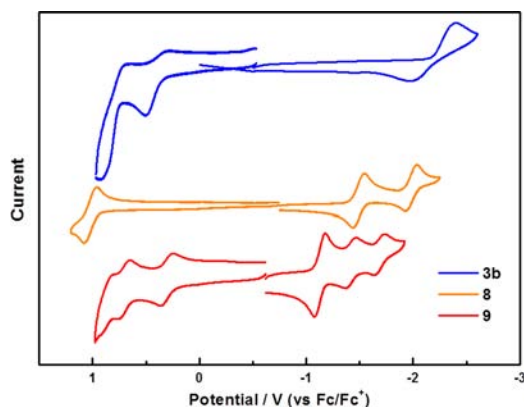


**Figure 5.** Cyclic voltammograms of **3b**, **8**, and **9** measured in  $\text{CH}_2\text{Cl}_2$ , except for the reduction process of **3b** in THF, with  $\text{Bu}_4\text{NPF}_6$  (0.1 M) at the scan rate of  $0.1 \text{ V s}^{-1}$ .

demonstrating its potential utility as a multielectron-accepting material. Compound **8** also shows two-step reversible redox processes for reduction. The  $E_{1/2}$  of  $-1.49 \text{ V}$  for the first reduction potential is much positively shifted from that of **7**. This difference demonstrates the inductive effect of the two carbonyl groups, which is also consistent with the DFT calculation results (vide supra). The calculation of this rigid skeleton at the B3LYP/6-311+G\*\* level gave the small reorganization energy of  $\lambda = 0.16 \text{ eV}$ , indicative of its potential as an n-type semiconducting material.

In summary, we succeeded in the synthesis of a series of new heterotriangulenes expanded with  $\text{C}=\text{C}$  or  $\text{C}=\text{O}$  double bonds and a fused polycyclic skeleton at the bridging moieties. The introduction of the 3-fold dibenzofluorenylidene bridges with highly twisted alkene conformations imparts not only the NIR absorption but also the multiredox properties up to a four-electron reduction. The modification of the heterotriangulene core into an unsymmetrical donor–acceptor skeleton with the dibenzochrysene substructure and the electron-withdrawing carbonyl groups gives rise to attractive properties including a fluorescence and a low reduction potential. These results should provide an important guideline for further designs of heterotriangulene-based  $\pi$ -conjugated materials, including more expanded nitrogen atom doped graphene flakes.

## ■ ASSOCIATED CONTENT

### Supporting Information

Experimental procedures, characterization data, and X-ray crystal structures (CIF) of **3a** (CCDC-990662), **7** (CCDC-990663), and **9** (CCDC-990918); photophysical properties, cyclic voltammograms, and theoretical calculations for all new compounds. This material is available free of charge via the Internet at <http://pubs.acs.org>.

## ■ AUTHOR INFORMATION

### Corresponding Author

\*E-mail: [yamaguchi@chem.nagoya-u.ac.jp](mailto:yamaguchi@chem.nagoya-u.ac.jp).

### Notes

The authors declare no competing financial interest.

## ■ ACKNOWLEDGMENTS

This work was supported by CREST, JST. C.-M.C. appreciates support of postdoctoral fellowships from the Japan Society for the Promotion of Science (JSPS).

## ■ REFERENCES

- (1) (a) Hellwinkel, D.; Melan, M. *Chem. Ber.* **1971**, *104*, 1001. (b) Hellwinkel, D.; Schmidt, W. *Chem. Ber.* **1980**, *113*, 358. (c) Filed, J. E.; Venkataraman, D. *Chem. Mater.* **2002**, *14*, 962.
- (2) (a) Wang, S.; Kivala, M.; Lieberwirth, I.; Kirchhoff, K.; Feng, X.; Pisula, W.; Müllen, K. *ChemPhysChem* **2011**, *12*, 1648. (b) Kivala, M.; Pisula, W.; Wang, S.; Mavrinskiy, A.; Gisselbrecht, J.-P.; Feng, X.; Müllen, K. *Chem.—Eur. J.* **2013**, *19*, 8117.
- (3) (a) Wan, X.; Zhang, H.; Li, Y.; Chen, Y. *New J. Chem.* **2010**, *34*, 661. (b) Zhang, H.; Li, Y.; Wan, X.; Chen, Y. *Chem. Phys. Lett.* **2009**, *479*, 117.
- (4) Zhang, H.; Wang, S.; Li, Y.; Zhang, B.; Du, C.; Wan, X.; Chen, Y. *Tetrahedron* **2009**, *65*, 4455.
- (5) (a) Fang, Z.; Zhang, X.; Lai, Y. H.; Liu, B. *Chem. Commun.* **2009**, 920. (b) Fang, Z.; Chellappan, V.; Webster, R. D.; Ke, L.; Zhang, T.; Liu, B.; Lai, Y.-H. *J. Mater. Chem.* **2012**, *22*, 15397.
- (6) (a) Bieri, M.; Blankenburg, S.; Kivala, M.; Pignedoli, C. A.; Ruffieux, P.; Müllen, K.; Fasel, R. *Chem. Commun.* **2011**, *47*, 10239. (b) Makarov, N. S.; Mukhopadhyay, S.; Yesudas, K.; Brédas, J.-L.; Perry, J. W.; Pron, A.; Kivala, M.; Müllen, K. *J. Phys. Chem. A* **2012**, *116*, 3781. (c) Schlütter, F.; Rossel, F.; Kivala, M.; Enkelmann, V.; Gisselbrecht, J.-P.; Ruffieux, P.; Fasel, R.; Müllen, K. *J. Am. Chem. Soc.* **2013**, *135*, 4550.
- (7) (a) Jiang, Z.; Chen, Y.; Yang, C.; Cao, Y.; Tao, Y.; Qin, J.; Ma, D. *Org. Lett.* **2009**, *11*, 1503. (b) Jiang, Z.; Ye, T.; Yang, C.; Yang, D.; Zhu, M.; Zhong, C.; Qin, J.; Ma, D. *Chem. Mater.* **2011**, *23*, 771.
- (8) (a) Do, K.; Kim, D.; Cho, N.; Paek, S.; Song, K.; Ko, J. *Org. Lett.* **2012**, *14*, 222.
- (9) (a) Kuratsu, M.; Kozaki, M.; Okada, K. *Angew. Chem., Int. Ed.* **2005**, *44*, 4056. (b) Suzuki, S.; Nagata, A.; Kuratsu, M.; Kozaki, M.; Tanaka, R.; Shiomi, D.; Sugisaki, K.; Toyota, K.; Sato, K.; Takui, T.; Okada, K. *Angew. Chem., Int. Ed.* **2012**, *51*, 3193.
- (10) (a) Takase, M.; Enkelmann, V.; Sebastiani, D.; Baumgarten, M.; Müllen, K. *Angew. Chem., Int. Ed.* **2007**, *46*, 5524. (b) Takase, M.; Narita, T.; Fujita, W.; Asano, M. S.; Nishinaga, T.; Bente, H.; Yoza, K.; Müllen, K. *J. Am. Chem. Soc.* **2013**, *135*, 8031.
- (11) In the course of this research, we learned that Kivala and co-workers have investigated related olefinated heterotriangulenes.
- (12) Korenaga, T.; Kosaki, T.; Fukumura, R.; Ema, T.; Sakai, T. *Org. Lett.* **2005**, *7*, 4915.
- (13) (a) Corey, E. J.; Fuchs, P. L. *Tetrahedron Lett.* **1972**, 3769. (b) Shun, A. L. K. S.; Tykwinski, R. R. *Angew. Chem., Int. Ed.* **2006**, *45*, 1034. (c) Donovan, P. M.; Scott, L. T. *J. Am. Chem. Soc.* **2004**, *126*, 3108.
- (14) (a) King, B. T.; Kroulik, J.; Robertson, C. R.; Rempala, P.; Hilton, C. L.; Korinek, J. D.; Gortari, L. M. *J. Org. Chem.* **2007**, *72*, 2279. (b) Grzybowski, M.; Skonieczny, K.; Butenschön, H.; Gryko, D. T. *Angew. Chem., Int. Ed.* **2013**, *52*, 9900.
- (15) Hayashi, Y.; Takeda, M.; Miyamoto, Y.; Shoji, M. *Chem. Lett.* **2002**, 414.
- (16) Allen, F. H.; Kennard, O.; Watson, D. G.; Brammer, L.; Orpen, A. G.; Taylor, R. *J. Chem. Soc., Perkin Trans. 2* **1987**, S1–S19.
- (17) (a) Kushida, T.; Camacho, C.; Shuto, A.; Irle, S.; Muramatsu, M.; Katayama, T.; Ito, S.; Nagasawa, Y.; Miyasaka, H.; Sakuda, E.; Kitamura, N.; Zhou, Z.; Wakamiya, A.; Yamaguchi, S. *Chem. Sci.* **2014**, *5*, 1296. (b) Kushida, T.; Yamaguchi, S. *Organometallics* **2013**, *32*, 6654.
- (18) Suzuki, T.; Fukushima, T.; Miyashi, T.; Tsuji, T. *Angew. Chem., Int. Ed.* **1997**, *36*, 2495.
- (19) Frisch, M. J. et al. Gaussian 09, revision C.01; Gaussian, Inc.: Wallingford, CT, 2010. See the Supporting Information for the full reference.
- (20) Buckminsterfullerene, C<sub>60</sub>, University of Bristol, Chm.bris.ac.uk (1996-10-13). Retrieved on 2011-12-25.